

Research Article

lncRNA GAU1 Induces GALNT8 Overexpression and Potentiates Colorectal Cancer Progression

Xuemei Tang ¹, Haoyu Ruan ¹, Liu Dong ¹, Sihao Li,² Zhiyuan Wu ¹,
and Ming Guan ¹

¹Department of Laboratory Medicine, Huashan Hospital, Shanghai Medical College, Fudan University, Shanghai 200040, China

²Center for Pharmacogenetics, Department of Pharmaceutical Sciences, University of Pittsburgh, PA 15261, USA

Correspondence should be addressed to Zhiyuan Wu; wuzhiyuan126@126.com and Ming Guan; guanming88@yahoo.com

Received 14 July 2020; Accepted 4 June 2021; Published 18 June 2021

Academic Editor: Michele Manigrasso

Copyright © 2021 Xuemei Tang et al. This is an open access article distributed under the Creative Commons Attribution License, which permits unrestricted use, distribution, and reproduction in any medium, provided the original work is properly cited.

lncRNA is a key epigenetic regulator in biological processes. In the human cancer transcriptome library MiTranscriptome, we identified *GAU1* as the top upregulated lncRNA in colorectal cancer (CRC) by sample set enrichment analysis (overexpression ranking percentile = 99.75%, $P < 10^{-50}$), which is coexpressed with the potential oncogene *GALNT8* (Spearman $\rho = 0.67$, $P = 2.44 \times 10^{-23}$, TCGA dataset $n = 184$). Experimental data revealed that *GAU1* regulates the expression of *GALNT8*. The overexpression of either *GAU1* or *GALNT8* significantly promotes the cell cycle and proliferation of CRC cell lines and correlates with poor prognosis in patients with CRC ($P = 3.04 \times 10^{-2}$), while silencing of *GAU1* or *GALNT8* suppressed the cancer cell proliferation and induced the CRC cell line resistance to oxaliplatin *in vitro* treatment. Our results suggested that the previously less studied *GAU1* and *GALNT8* may play as CRC prognosis markers and potential targets for chemotherapy treatment.

1. Introduction

Colorectal cancer (CRC) ranked the third common type of cancer, adding up 10% of all cases [1]. In 2018, there were over one million new cases and over half million deaths from the disease [2]. Genetic mutations in *APC* [3], *TP53* [4], and *K-RAS* [5] have been intensively studied as major contributors to the tumorigenesis of CRC. Besides, nongenetic risk factors like aging and lifestyle also induce the development of CRC cases. However, this nonmutational alteration in CRC was less studied [6]. Massive parallel sequencing facilitated the genome-wide characterization of the human cancer transcriptome and identified long noncoding RNA (lncRNA) expression as the most common transcriptional alteration in cancer [7]. Our previous reports revealed that lncRNAs are extensively involved in the CRC development [8] and drug resistance [9], indicating that more efforts should be encouraged to identify the CRC-specific lncRNA

expression and to link the biological “operator” regulating these noncoding “regulators.”

RNA-Seq technology empowered by sequence alignment and assembly provides a revolutionary approach for the prediction of full-length transcripts from both the intergenic “gene desert” and protein-coding loci [10, 11]. The MiTranscriptome database applied *ab initio* assembly to 7,256 curated RNA-Seq libraries from tumor, normal tissue, and cell lines so as to provide an unbiased method for gene discovery [12]. Here, by incorporating this *ab initio* assembly-based human cancer transcriptome database and experimental validation, we identified a colorectal cancer-related lncRNA *GAU1* from 12,382 cancer-associated lncRNA transcripts and verified its pro-cancer function as upregulating the mRNA expression of polypeptide N-acetylgalactosaminyl transferase *GALNT8*, whose overexpression correlates with the cancer cell proliferation and poor patient survival.

2. Materials and Methods

2.1. Identification of *GAU1* as the CRC-Related lncRNA. The normalized counts of 12,382 ab initio-assembled lncRNA transcripts and library information of 6,476 RNA-Seq libraries (5,724 cancer-related samples and 752 normal samples) including 5,602 TCGA cases were downloaded from the MiTranscriptome website (<http://MiTranscriptome.org/download/MiTranscriptome.expr.counts.tsv.gz>).

Sample set enrichment analysis (SSEA) [12] was performed to test if a transcript is differentially expressed between the cancer and noncancer samples in an empirical ranking method. In brief, a weighted KS test was performed as gene set enrichment analysis (GSEA) [13] to generate the enrichment score (ES) describing the enrichment of the sample set among all tested samples. SSEA was further performed 1,000 times with random permutation of the ample labels for a set of null ES and the nominal *P* value of relative rank of observed ES within the null ES. The hypothesis testing was performed by comparing the tested ES to the null normalized enrichment score (NES) for all transcripts in a sample set. SSEA percentile score was generated by ranking the transcripts in each analysis by their NES. The tissue-type information of each transcript was obtained from the MiTranscriptome browser (<http://MiTranscriptome.org>).

To perform *GAU1* coexpression analysis, the normalized RSEM-FPKM mRNA expression of 382 TCGA CRC samples was obtained from TCGA firehose legacy (<https://gdac.broadinstitute.org/>). After sample overlapping with the MiTranscriptome database, Spearman's rank correlation coefficient of *GAU1* and all 19,815 protein-coding gene mRNA expression was calculated in 184 TCGA CRC samples.

2.2. Clinical Samples and Tissue Microarray. Primary CRC tissues and paired adjacent tissues were collected from 66 CRC patients. All these samples were obtained between 2015 and 2017 and stored at -80°C .

Tissue microarrays (TMAs) with 55 paired cases of CRC and adjacent nontumorous tissues, plus 14 individual CRC tissues, were obtained from Shanghai Tenth Hospital (Shanghai, PR China). These CRC specimens were collected from CRC patients between 2010 and 2015 and followed until April 2019. No patient received chemotherapy or radiation before surgery, and no other concurrent cancer was observed in the patients. Both the Institutional Review Boards of Shanghai Tenth Hospital and Huashan Hospital, Fudan University, approved our study in compliance with Helsinki Declaration of 1975 as revised in 1996. All patients signed the informed consent before surgical operation. The clinical stages were classified by the American Joint Committee on Cancer and Union for International Cancer Control (AJCC/UICC) classification system [14]. Overall survival (OS) is defined as the time interval between the date of surgery and death.

2.3. Cell Culture and Stable Cell Line Establishment. Human embryonic kidney cell line HEK293T and human colon/rectum cancer cell lines LoVo, DLD1, SW620, and HCT116 were purchased from Shanghai Institute of Biological Sci-

ences. All cell lines were maintained in Dulbecco's modified Eagle's medium (DMEM) (Gibco, CA, USA) with 10% FBS (Gibco) at 37°C in an atmosphere of 5% CO_2 .

The *GALNT8* ORF sequence (NM_017417.2) and *GAU1* (NR_110112.1) were cloned by reverse-transcriptional PCR from human mRNA and were further integrated into the lentiviral expression vector pCDH (Addgene, #72265) to develop pCDH-*GALNT8* and pCDH-*GAU1* recombinant plasmid. Lentivirus with *GALNT8* or *GAU1* overexpression vector or pCDH control vehicle was packaged with packaging plasmid psPAX2 (Addgene, #12260) and envelope plasmid pMD2.G (Addgene, #12259) using Lipofectamine 2000 (Invitrogen, #11668019) in HEK293T. Stable cell lines overexpressing *GALNT8*, *GAU1*, or vehicle control were established with SW620 and HCT116 cell lines by lentivirus infection.

2.4. siRNA Interference. siRNAs targeting *GALNT8* (si-*GALNT8*), *GAU1* (si-*GAU1*), and nonsense scramble (siNS) were purchased from Tuoran Biotech (Shanghai, China). The siRNA sequence is as follows: si-*GAU1*-1: 5'-CCAAGA ACUUCGGAAGCAUTT-3', si-*GAU1*-2: 5'-CCAGCUUAC ACGUCAGCUUTT-3', si-*GALNT8*-1: 5'-CUCGAUUGU UGAAGGAAAU-3', si-*GALNT8*-2: 5'-GCUCACAGAAU GUCUACUA-3', and siNS: 5'-UCCTAAGGUUAAGUCG CCUC-3'. siRNA transfection of LoVo, DLD1, and their derived *GAU1*-overexpressing cells or vehicle control cells was undertaken with Lipofectamine RNAiMax (Invitrogen, #13778150). All the cancer cell line transfection was performed 48 hours before further experimental usage.

2.5. Cell Proliferation and Cell Cycle Assay. Cancer cell lines were seeded 1×10^3 per well in the 96-well plate. The cell proliferation was assessed by Cell Counting Kit-8 (CCK8, MCE, #HY-K0301) every 24 hours for 5 days. The colony formation ability of cancer cell lines was measured by 0.1% crystal violet/methanol staining 10 days after cell seeding in six-well plates at 1×10^3 per well density. Any colony that contains more than 50 cells was counted.

Cell cycle analysis was performed with Propidium Iodide (PI) staining. A total of 10^6 cells were rinsed twice with cold PBS, then fixed with 75% ethanol overnight at -20°C , rinsed three times with PBS, and resuspended with 0.5 ml FxCycle™ PI/RNase Staining Solution (Life Technologies, #F10797). Keep the cell suspension for 15 min in the dark, and immediately subject to flow cytometry analysis on a FACSCanto system (BD Biosciences).

2.6. Quantitative Real-Time PCR. Trizol reagent (Invitrogen) was used for total RNA of tissues or cell extraction. Reverse transcription was performed with PrimeScript™ RT Reagent Kit (TaKaRa Biotechnology, #RR047A). Quantitative real-time PCR was conducted with TB Green Premix (TaKaRa Biotechnology, #RR820A) and gene-specific primers (Table 1) on an Applied Biosystems 7500 system (ABI); β -actin was used as a mRNA expression housekeeping gene (Table 1). Relative expression of *GALNT8* and *GAU1* was calculated with the $2^{-\Delta\Delta\text{Ct}}$ method.

TABLE 1: Primer sequences for gene amplification.

Gene	Strand	Sequences (5'-3')
GALNT8	Forward	ACGCCCTCTCGATTGTTGAA
	Reverse	CTCTGCCACCCAACATTGA
GAU1	Forward	GCCCTTCCCAAAGCACAAAT
	Reverse	AGCACGTTAAGAGGCTTGGA
β -Actin	Forward	TTGTTACAGGAAGTCCCTTGCC
	Reverse	ATGCTATCACCTCCCCTGTGTG

2.7. Antibody and Regent Information. The primary antibodies are GALNT8 (Abcam, #ab121374) and β -actin (Cell signaling technology, #3700). The secondary antibodies are HRP-labeled goat anti-rabbit IgG (Thermo Fisher, #31460) and HRP-labeled goat anti-mouse IgG (Thermo Fisher, #31430). Oxaliplatin was purchased from MCE (#HY-17371).

2.8. Protein Isolation and Immunoblotting. Cancer cell samples were suspended with 0.05% trypsin and washed twice with cold PBS and, after, homogenized with RIPA lysis buffer and protease inhibitor cocktail (Beyotime Biotechnology, #P0013D) on ice for 30 minutes. Cell lysates were harvested by 4°C centrifuge and diluted with 2× SDS sample buffer. The denatured protein samples were resolved by SDS-PAGE and transferred onto polyvinylidene fluoride (PVDF) membranes (Millipore, #ISEQ00010). Blocked with 5% skimmed milk in PBST, the PVDF membranes were incubated with specific primary antibodies overnight at 4°C. After 3 times of 10-minute TBST buffer rinsing, the membranes were again incubated with secondary antibodies for 1 hour at room temperature and rinsed 3 times with TBST buffer for 10 minutes. Signals were detected with enhanced chemiluminescence (ECL) substrate (ThermoFisher, #32106) on a Las-3000 Luminescent Image Analyzer (Fujifilm, Japan).

2.9. TMA Staining and Immunohistochemistry. The TMA slide was air-dried at 60°C for an hour and treated with 0.01 M citric acid buffer solution for antigen retrieval. After cooling down to room temperature, the slide was further treated by 3% H₂O₂ solution in methanol for 10 minutes and rinsed 3 times with cold PBS before incubation with primary anti-GALNT8 antibody (1:100) at 4°C overnight. The slides were rinsed three times for 5 minutes and then incubated with ready-to-use biotinylated goat anti-rabbit IgG (Abcam, #ab64256) solution for 15 minutes at room temperature, followed by PBS rinsing for five times. Streptavidin peroxidase complex (Abcam, #ab64269) was applied to the TMA and incubated for 10 minutes at room temperature and rinsed by PBS for five times. After visualization with diaminobenzidine chromogen (Abcam, #ab64238) and hematoxylin counterstaining, the TMA was imaged using a Nikon Eclipse E-800 microscope. The stained TMA was then independently reviewed by two pathologists and rated for the grade of GALNT8 staining with scores of -, +/-, +, ++, and +++.

2.10. Cytotoxic Assay. For SW620 and DLD1, the cells with manipulated GAU1 expression or control were seeded in the 96-well plate at a density of 1×10^3 cells per well and incubated with low serum medium (1% v/v FBS) with or without oxaliplatin. Cells were replenished with fresh low serum medium with or without oxaliplatin on the third day. Cell Counting Kit-8 (CCK8, MCE, #HY-K0301) assay was used to estimate the cell viability at the end of the fifth day of treatment.

2.11. Subcellular Isolation. Subcellular isolation in LoVo and DLD1 cells was performed as described [15] with modification. Prepare isolation buffer (1.28 M sucrose; 40 mM Tris-HCl, pH 7.5; 20 mM MgCl₂; and 4% Triton-X 100) and diluted isolation buffer (cold H₂O : cold PBS : isolation buffer = 3 : 1 : 1). 10⁶ cells were suspended in 200 μ l diluted isolation buffer and incubated on ice for 10 min. 20 μ l lysate was added to 1 ml Trizol for total RNA extraction. The rest of the lysate was rotated at 4°C for 20 min and centrifuged at 2500 × g for 15 min at 4°C. Add 1 ml Trizol to the supernatant for cytoplasmic RNA extraction. Wash the pellet once, resuspend with 160 μ l isolation buffer, and add 1 ml Trizol for the nuclear RNA extraction. Fractionated RNAs were used for cDNA synthesis and qRT-PCR.

2.12. Statistical and Survival Analysis. GraphPad Prism 7 (La Jolla, CA, USA) and SPSS 20 (IBM, NY) were used for statistical analysis and graph preparation. All data are displayed as means \pm SD. Two-tailed Student's *t*-test was used for assessment of differences between any two groups. Kaplan-Meier analysis was used to perform survival analysis, and the patients' survival comparison between subgroups was analyzed with log-rank test. Nonparametric Wilcoxon-Mann-Whitney test was performed for patients' clinical data analysis.

3. Results

3.1. Identification of GAU1 as the Colorectal Cancer-Related lncRNA. To identify the colorectal cancer-related lncRNA in the MiTranscriptome database, we first performed the differential expression analysis for all the 5,724 cancer libraries vs. 752 noncancer libraries by SSEA and annotated all the transcripts with tissue-type information (Figure 1(a)). After the empirical ranking test, two transcripts of GAU1 (ENSG00000255474) were listed on the top CRC-related lncRNA (ranking percentile = 99.75% of 12,382) besides our previously reported CRC-specific lncRNA *PHiL* [9] (ranking percentile = 99.62%).

Then, we further experimentally quantified the GAU1 mRNA overexpression in human colorectal cancer cell lines SW620, HCT116, DLD1, and LoVo versus human intestinal epithelial cell line NCM460 ($P < 0.05$, Figure 1(b)). Furthermore, qRT-PCR of GAU1 mRNA in 66 pairs of CRC tissues and adjacent normal tissues also confirmed GAU1 as the cancer-specific lncRNA in CRC ($P = 2.53 \times 10^{-2}$, Figure 1(c)). More importantly, the Kaplan-Meier analysis revealed that patients with higher GAU1 expression had worse prognosis ($P = 3.04 \times 10^{-2}$, Figure 1(d)), indicating GAU1 may play an oncogenic role in CRC. And the

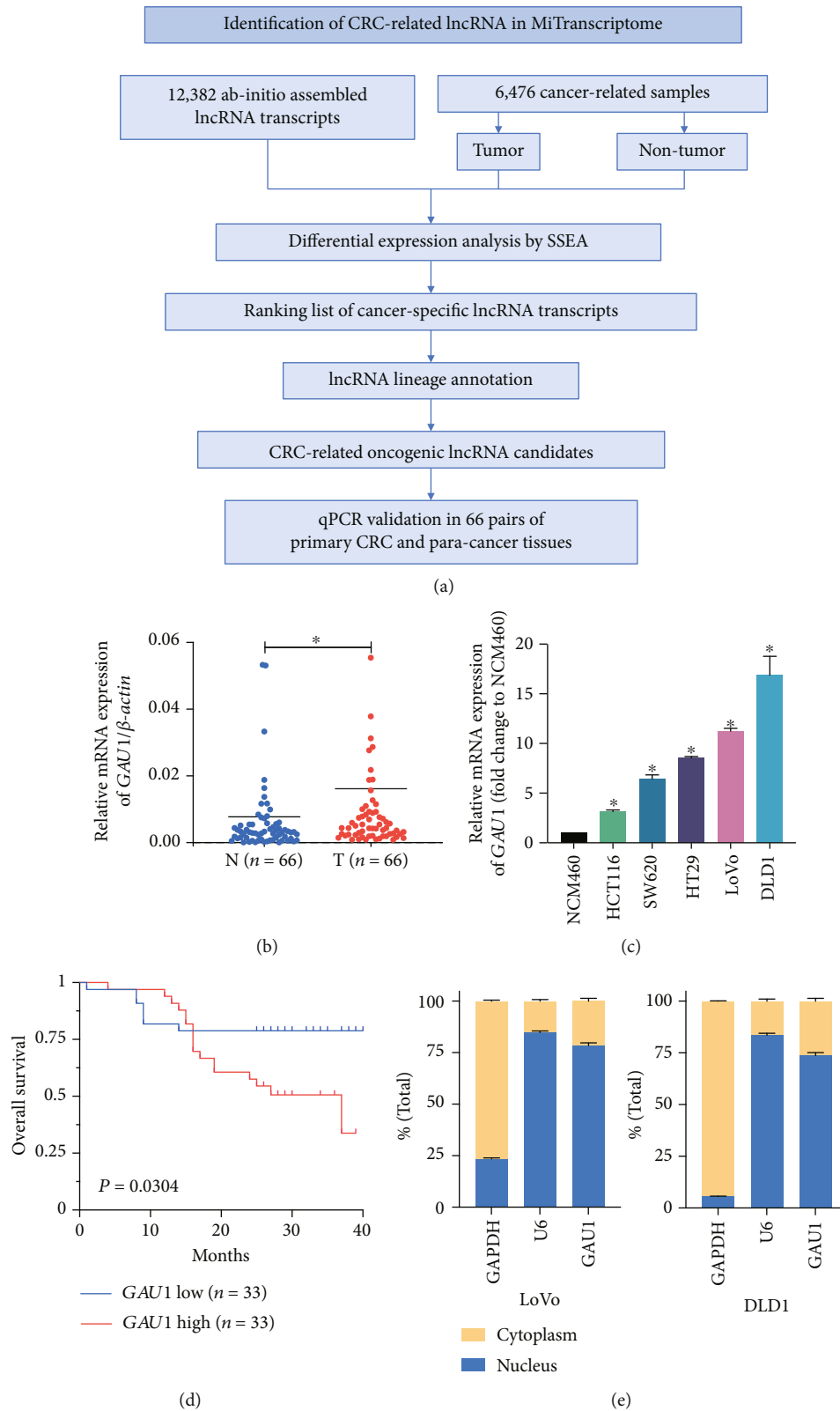


FIGURE 1: Identification of *GAU1* as the colorectal cancer-related lncRNA. (a) The working pipeline of identifying CRC-related lncRNA in the MiTranscriptome database. (b) Relative expression level of *GAU1* detected by qRT-PCR in 66 paired colorectal cancer (CRC) tissues and adjacent normal tissues ($P = 2.53 \times 10^{-2}$). N: adjacent normal tissues; T: tumor tissues. (c) qRT-PCR analysis of *GAU1* expression in the five CRC cell lines and the normal NCM460 cells was tested. $*P < 0.05$. (d) Kaplan-Meier analysis of the correlation between *GAU1* mRNA expression and overall survival in 66 CRC patients ($P = 3.04 \times 10^{-2}$). (e) Total RNA from LoVo and DLD1 cells was separated into cytoplasmic and nuclear fractions and analyzed by qRT-PCR. GAPDH serves as a positive control for cytoplasmic gene expression, and U6 as a positive control for nucleolus separation.

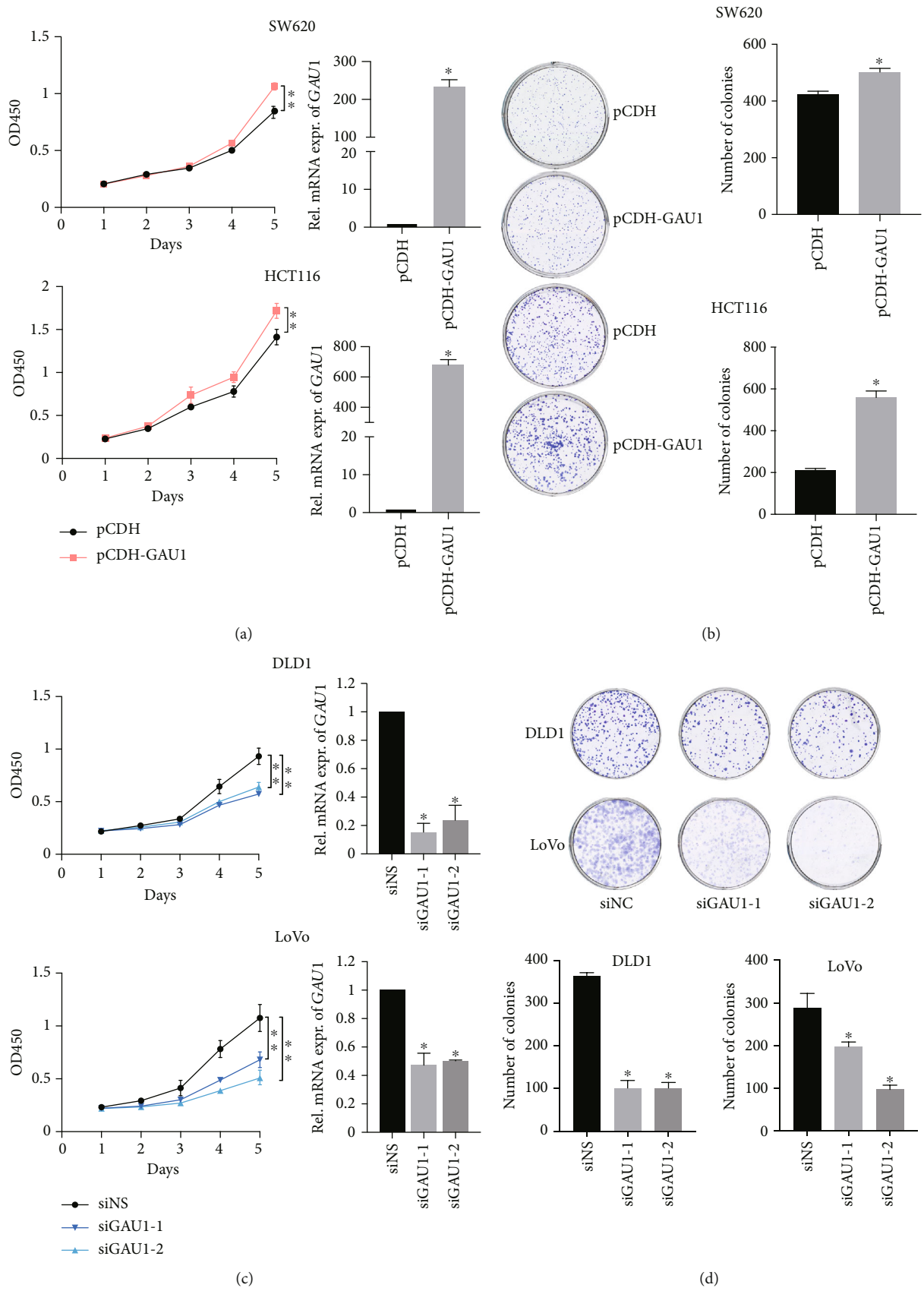
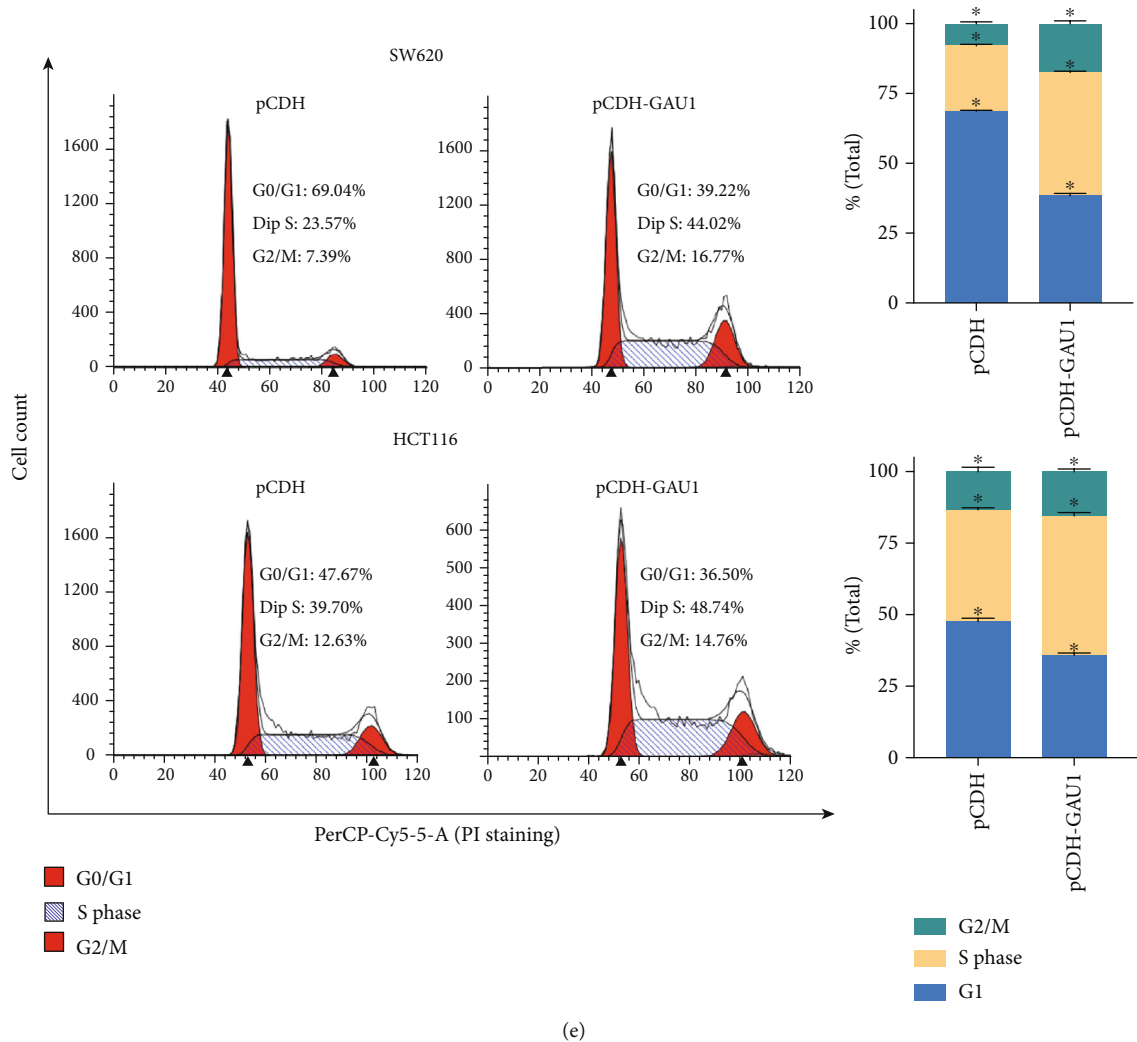


FIGURE 2: Continued.



(e)

FIGURE 2: *GAU1* overexpression facilitates CRC cell proliferation. (a) CCK-8 assay and (b) colony formation assay were conducted in SW620 and HCT116 cells transfected with *GAU1* overexpression or control plasmids. * $P < 0.05$; ** $P < 0.01$. (c) CCK-8 assay and (d) colony formation assay showed the proliferation of control siRNA (siNS) or siRNAs (siGAU1-1 and siGAU1-2) against *GAU1*-transfected DLD1 and LoVo cells. * $P < 0.05$; ** $P < 0.01$. (e) Cell cycle analysis of *GAU1*-overexpressed HCT116, SW620, and their controls.

subcellular localization showed that *GAU1* was mainly distributed in the nucleus (Figure 1(e)).

3.2. *GAU1* Overexpression Facilitates CRC Cell Proliferation by Promoting Cell Cycle. To further determine if the *GAU1* overexpression can alter the biological phenotype of CRC, we first established the *GAU1*-overexpressing stable cell lines by lentiviral infection of pCDH-*GAU1* in SW620 and HCT116 cell lines with intermediate *GAU1* expression. The CCK-8 and clonogenic assays both revealed that *GAU1* overexpression lead to a significantly increased cell proliferation in the CRC cell lines compared to the vehicle controls (Figures 2(a) and 2(b)). Consistently, *GAU1* knockdown in the *GAU1* high-expressing LoVo and DLD1 cell lines by short interfering RNA (siRNA) significantly reduced the cell proliferation and clonogenic ability of the CRC cells (Figures 2(c) and 2(d)). These data suggested that *GAU1* overexpression promotes CRC cell proliferation in vitro. Moreover, the cell cycle profile alteration after *GAU1* overex-

pression (increased S-phase commitment) (Figure 2(e)) also implied *GAU1* as a critical player in promoting S-phase entry.

3.3. *GALNT8* as the Oncogenic Operator of *GAU1* in CRC. To identify the biological “operator” of *GAU1* overexpression in CRC development, we performed coexpression analysis for *GAU1* in 184 TCGA CRC samples. Correlation analysis revealed *GALNT8*, located in the vicinal gene loci of *GAU1* on chromosome 12, as the most significantly coexpressed gene of *GAU1* among all the 19,815 protein-coding genes (Spearman $\rho = 0.67$, $P = 2.44 \times 10^{-23}$, Figure 3(a)). The strong expression correlation between *GAU1* and *GALNT8* was further validated in our 66 pairs of clinical samples ($P < 10^{-4}$, Figure 3(a)), with a significant upregulation of *GALNT8* expression in the tumor tissues (T) compared with the adjacent nontumorous tissues (N) ($P < 10^{-4}$, Figure 3(b)). Clinically, the Kaplan-Meier analysis also revealed that patients with higher *GALNT8* expression had worse overall survival ($P = 0.31 \times 10^{-2}$, Figure 3(c)).

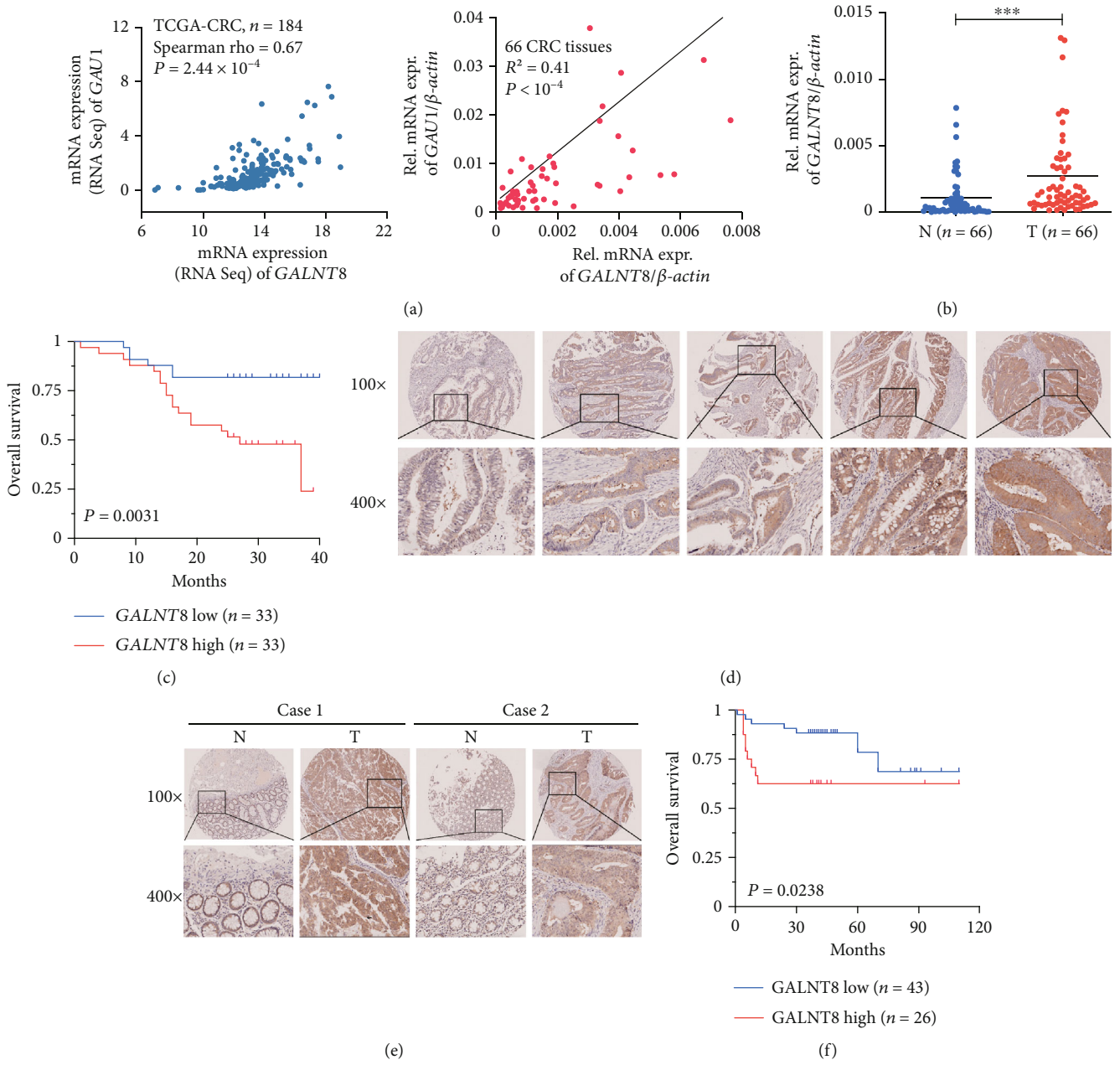


FIGURE 3: Continued.

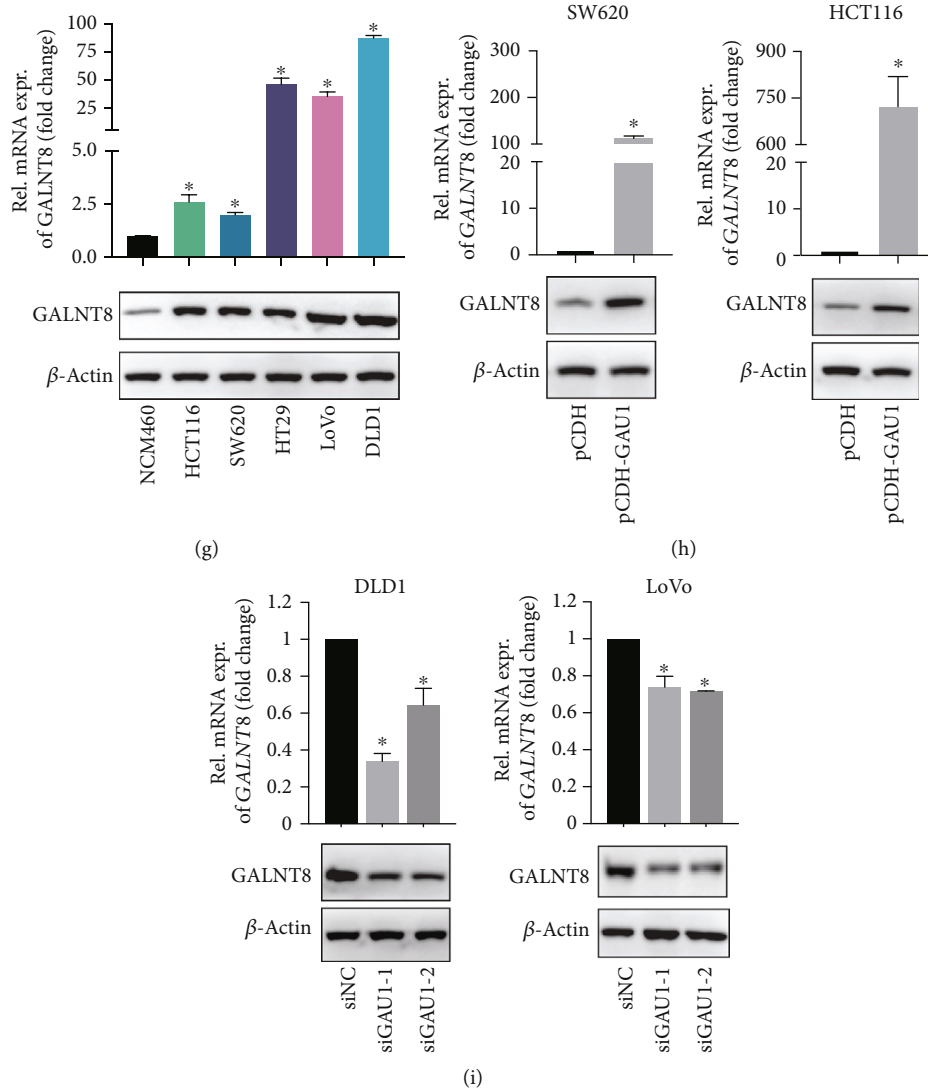


FIGURE 3: GALNT8 as the oncogenic operator of *GAU1* in CRC. (a) Correlation analysis of *GALNT8* and *GAU1* in 184 TCGA CRC samples (Spearman $\rho = 0.67$, $P = 2.44 \times 10^{-23}$), and 66 frozen CRC tissues (qRT-PCR, $R^2 = 0.41$, $P < 10^{-4}$). (b) qRT-PCR analysis of *GALNT8* expression level in 66 paired CRC tissues and adjacent normal tissues ($P < 10^{-4}$). N: adjacent normal tissues; T: tumor tissues. (c) Kaplan-Meier analysis of *GALNT8* and overall survival in 66 CRC patients. (Kaplan-Meier $P = 0.31 \times 10^{-2}$). (d) Representative photomicrographs of *GALNT8* in CRC specimen TMA (magnification: $\times 100$, $\times 400$). (e) Two paired tumor-adjacent control representative cases of *GALNT8* expression in the TMA (magnification: $\times 100$, $\times 400$). (f) Kaplan-Meier analysis of *GALNT8* expression and overall survival in 69 TMA samples. (Kaplan-Meier $P = 2.38 \times 10^{-2}$). (g) qRT-PCR and western blot analysis of *GAU1* expression in the five CRC cell lines and the normal NCM460 cells was tested. * $P < 0.05$. (h) qRT-PCR and western blot analysis of *GALNT8* expression level in *GAU1*-overexpressed SW620 and HCT116 cells, as well as (i) *GAU1*-knockdown DLD1 and LoVo cells. * $P < 0.05$.

The overexpression of *GALNT8* in the CRC patients was further validated by the IHC staining of a TMA containing 55 paired cases of CRC and adjacent nontumorous tissues, plus 14 individual CRC tumors. According to the density of IHC staining (Figure 2(d)), *GALNT8* protein expression in tumor tissues was classified as high expression (score ++, score +++) in 26 cases (26/69, 37.68%) and low expression (score +, score +/-, and score -) in 43 cases (43/69, 62.32%) (Figure 3(d)). Tumor tissues harbored a significantly increase *GALNT8* expression compared to the adjacent nontumorous tissues (Fisher exact $P = 3.30 \times 10^{-8}$, Figure 3(e)). Further survival assay by Kaplan-Meier analysis also revealed that

CRC patients with overexpressed *GALNT8* suffered from poor overall survival ($P = 2.38 \times 10^{-2}$, Figure 3(f)).

Moreover, in contrast to human intestinal epithelial cell line, a higher expression of *GALNT8* in CRC cells was observed in both mRNA and protein levels (Figure 3(g)). To further confirm the regulatory effect of *GAU1* on *GALNT8* expression, the effect of *GAU1* knockdown/overexpression on the expression levels of *GALNT8* in CRC cells was determined. The mRNA and protein expression levels of *GALNT8* were increased in the *GAU1* overexpression cell lines and decreased in the si*GAU1* cell lines compared with the control group (Figures 3(h) and 3(i)). Altogether, the

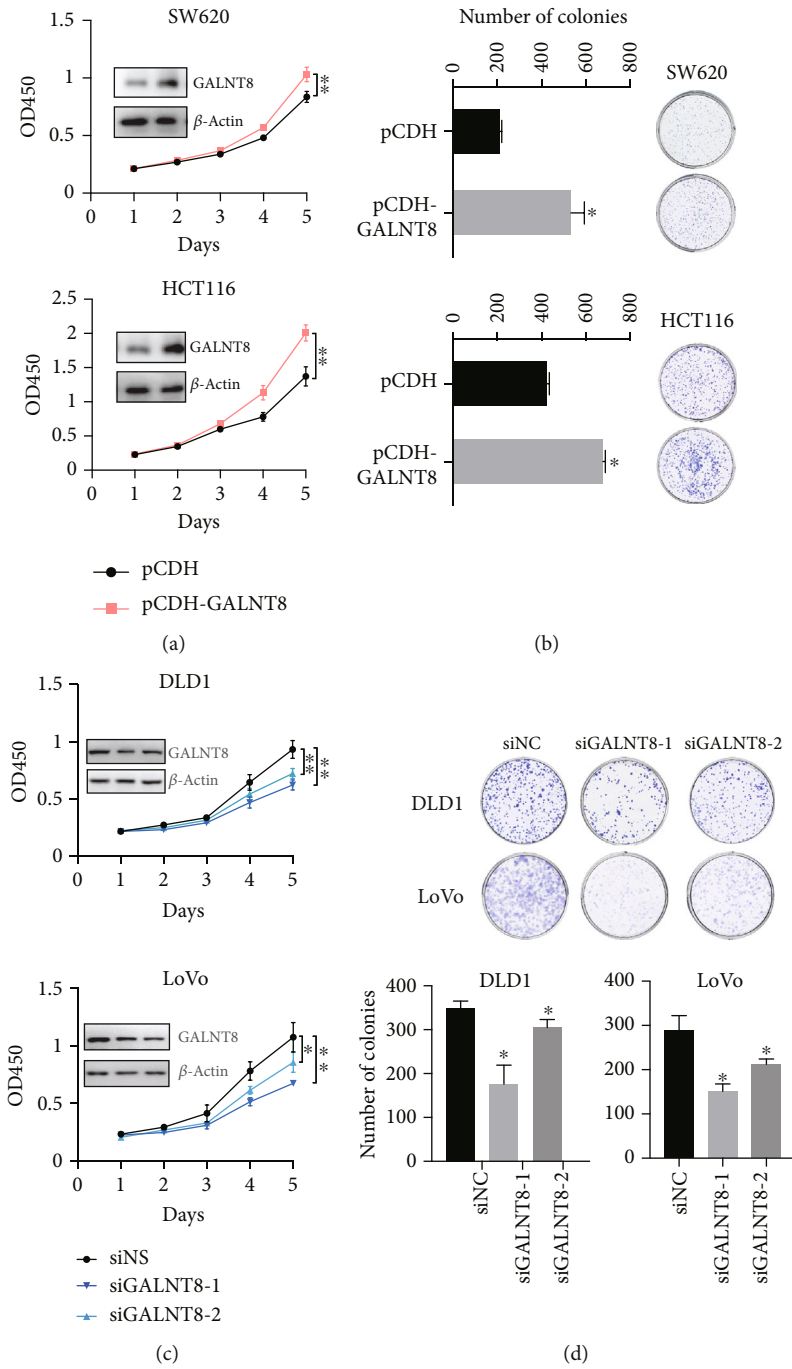


FIGURE 4: Continued.

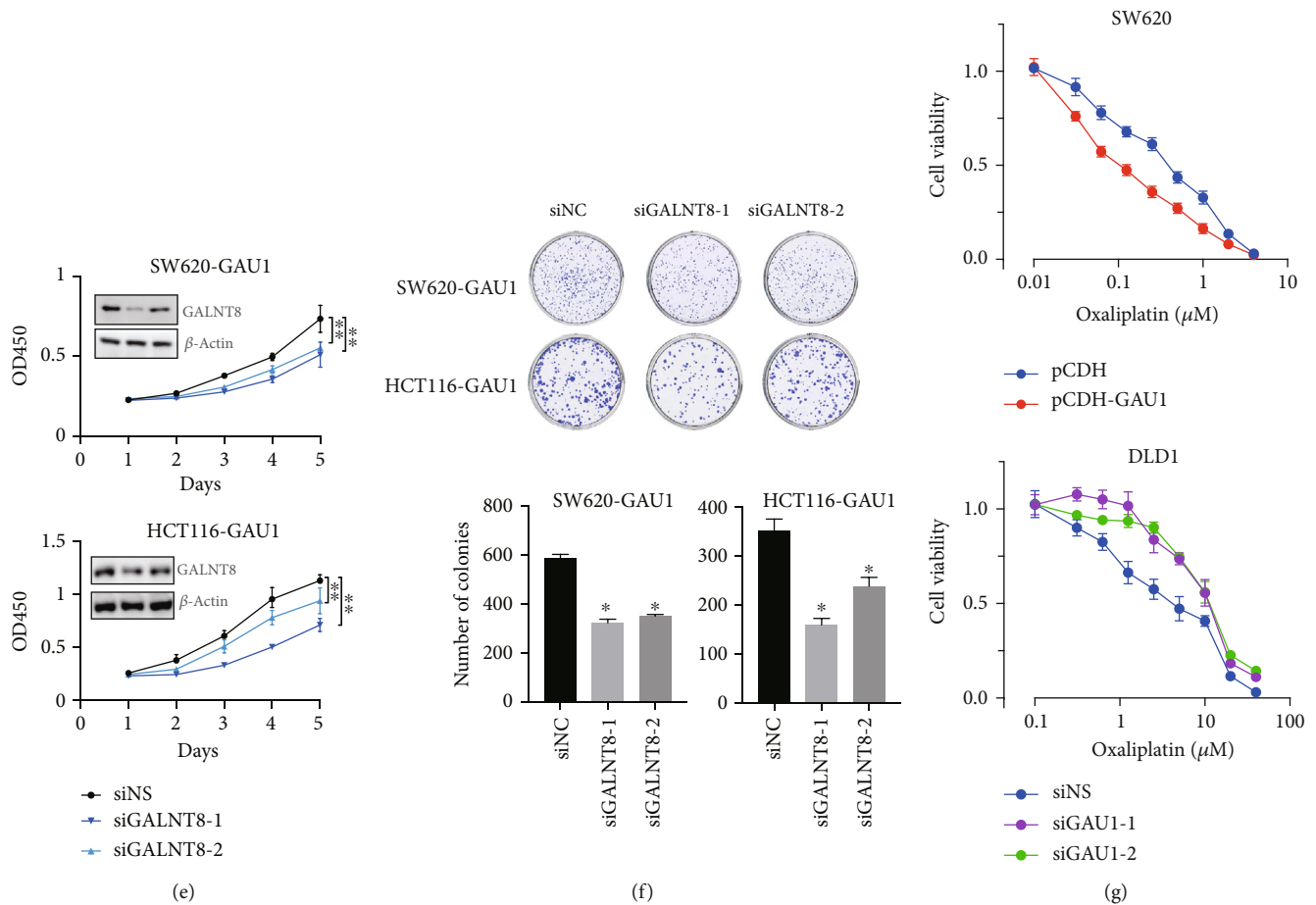


FIGURE 4: The oncogenic ability of *GAU1* is *GALNT8* dependent, and overexpression of *GAU1*/*GALNT8* axis sensitizes CRC cell lines to chemotherapy. (a) CCK-8 assay and (b) colony formation assay were used to measure proliferation in SW620 and HCT116 cells transfected with pCDH-*GALNT8* or pCDH. * $P < 0.05$; ** $P < 0.01$. (c) CCK-8 assay and (d) colony formation assay were conducted in control siRNA (siNS) or siRNAs (siGALNT8-1 and siGALNT8-2) against *GALNT8*-transfected DLD1 and LoVo cells. * $P < 0.05$; ** $P < 0.01$. (e, f) Proliferation analysis by (e) CCK-8 assay and (f) colony formation assay in *GAU1*-overexpressed SW620 and HCT116 cells transfected with control siRNA (siNS) or siRNAs (siGALNT8-1 and siGALNT8-2) against *GALNT8*. * $P < 0.05$; ** $P < 0.01$. (g) Viability of pCDH-*GAU1*- or pCDH-transfected SW620 and siGAU1-1/2- or siNS-transfected DLD1 cells incubated with multiple concentrations of oxaliplatin (0.01–40 μ M) was monitored through CCK-8 assay.

computational and experimental evidence suggested *GALNT8* as a regulatory downstream molecule of *GAU1* in CRC.

3.4. The Oncogenic Ability of *GAU1* Is *GALNT8* Dependent.

Since the relationship between *GALNT8* and cancer is limited, we experimentally manipulated the expression of *GALNT8* by lentiviral stable overexpression and siRNA interference. CCK-8 and colony forming assays demonstrated that the overexpression of *GALNT8* enhanced the proliferation and colony formation capacity of SW620 and HCT116 (Figures 4(a) and 4(b)), whereas the contrary results were observed in the *GALNT8*-suppressed DLD1 and LoVo cell lines (Figures 4(c) and 4(d)). With all these results, it is suggested that *GALNT8* contributes to CRC cell proliferation.

To further explore the oncogenic partnership of the *GAU1*/*GALNT8* cluster in CRC, siGALNT8 or negative control was transfected into *GAU1*-overexpressing cell lines to examine whether *GALNT8* silence could rescue *GAU1* overexpression-mediated enhanced proliferation of CRC.

The CCK-8 and colony formation assay results demonstrated that the upregulated cell proliferation and colony formation in the *GAU1*-overexpressed SW620 and HCT116 cell lines were partially attenuated by siGALNT8 in Figures 4(e) and 4(f)), suggesting that *GALNT8* is a critical downstream operator of *GAU1* during the CRC proliferation.

3.5. Overexpression of *GAU1*/*GALNT8* Axis Sensitizes CRC Cell Lines to Chemotherapy.

Given the experimental evidence that *GAU1*/*GALNT8* axis overexpression significantly promotes the cancer cell proliferation and *GAU1* boosts cell cycle by increasing S-phase entry, we further questioned if *GAU1*/*GALNT8* axis can reshape the drug response of cancer cells to chemotherapy agents targeting DNA replication. The *in vitro* oxaliplatin drug response data revealed that cancer cells overexpressing *GAU1* or *GALNT8* are more vulnerable to chemotherapy agents causing replication fork collapse, indicating *GAU1*/*GALNT8* axis as a potential actionable target for the personalized medicine of CRC. This finding was

further confirmed by the drug resistance phenotype in *GAU1/GALNT8* knockdown cell lines (Figure 4(g)).

4. Discussion

CRC is one of the most common and lethal types of cancer [16]. In the past decades, genetic alteration including *APC* and *K-RAS* somatic mutation has been identified to cause 70% of the CRC cases [17] and widely adapted into the diagnosis and drug response prediction during CRC management [18].

Recent studies attributed the transcriptional alteration of the lncRNAs as a hallmark of tumor development [19, 20]. The enormous efforts on the landscaping of lncRNA expression in cancer [21, 22] led to a number of fabulous investigations that improved the understanding of multiple major cancer types [7].

In this study, we identified *GAU1* as one of the major oncogenic lncRNAs for CRC by mining the ab initial strategy-based lncRNA database MiTranscriptome [10, 11]. According to our analysis, *GAU1* ranked one of the most differentially expressed lncRNAs between CRCs and normal tissues/cell lines (99.75% percentile of SSEA). Moreover, the overexpression of *GAU1* leads to a significant reduction in CRC patient survival ($P = 3.04 \times 10^{-2}$). After experimentally validating the procancerous ability of *GAU1* by the cell proliferation assay after *GAU1* expression manipulation in CRC cell lines, we further located *GALNT8* as the mostly coexpressed protein-coding gene for *GAU1*.

GALNT8 encodes a 637-amino-acid type-II membrane protein (GalNAc-T8) [23]. The protein is a member of the UDP-GalNAc polypeptide N-acetylgalactosaminyl transferase (ppGaNtase) family, which initiates mucin-like O-linked protein glycosylation in the Golgi apparatus [24]. Previous research revealed that *GALNT8* is expressed in the heart, placenta, skeletal muscle, liver, and kidney and plays a key role during embryonic development [23]. However, the oncogenic effect of *GALNT8* is less characterized. Chai et al. reported *GALNT8* as the oncogene in retinoblastoma that potentially drives the cancer development and progression [25] by directly binding to the *GALNT8* promoter and boost the transcription of *GALNT8* through TCEA1 (Transcription Elongation Factor A1) recruitment, which mechanistically endorsed our experimental data in CRC.

Like *GAU1*, *GALNT8* is also associated with poor CRC prognosis ($P = 0.31 \times 10^{-2}$). Together with the experimental evidence (1) overexpression or silencing *GALNT8* mimicked the cancer cell line phenotypic alteration after *GAU1* overexpression or knockout. (2) *GALNT8* knockdown attenuated the *GAU1* overexpression-induced cell proliferation, and not vice versa; we confirmed *GALNT8* as the downstream operator of *GAU1* in CRC.

Aside from the surgical operation, systemic chemotherapy with folinic acid, fluorouracil, and oxaliplatin (FOLFOX) is also a main treatment solution for CRC. Our result showed an oxaliplatin hypersensitivity in cancer cell lines overexpressing *GAU1/GALNT8*. This double-edge sword effect of *GAU1/GALNT8* overexpression suggested the *GAU1/GALNT8* axis as a potential marker in the precision medicine

of CRC, although more experimental evidence should be investigated in the future.

One limitation of this study is we did not provide the molecular interaction between *GAU1* and *GALNT8*. Although we have confirmed *GALNT8* as the essential operator for the oncogenic ability of *GAU1*, further investigation on the regulatory mechanism between these bidirectionally transcribed lncRNA/protein-coding gene pairs needs to be clarified by protein-RNA interaction or DNA-RNA binding assay. According to the previous report that *GAU1* and *GALNT8* share a cisregulation relationship in retinoblastoma [25] and the mutual promoter region of the two genes, investigation on the mechanism behind the abnormal promoter activation in CRC should be conducted in our future studies.

To our best knowledge, this is the first study systematically reporting the oncogenic cascade of *GAU1/GALNT8* axis in CRC. By integrating the differential expression data from 7,256 curated RNA-Seq libraries in MiTranscriptome and experimental validation, we demonstrated that *GAU1*, together with its downstream protein *GALNT8*, is associated with cancer cell proliferation, poor patient survival, and chemotherapy response.

Data Availability

The data used to support the findings of this study are included within the article.

Conflicts of Interest

The author(s) declare(s) that they have no conflicts of interest.

Authors' Contributions

Xuemei Tang and Haoyu Ruan contributed equally to this article.

Acknowledgments

This study was supported by the National Natural Science Foundation of China (81871728 and 81672105 to M.G., 81802993 to Z.W.) and Innovation Group Project of Shanghai Municipal Health Commission (2019CXJQ03 to M.G.).

References

- [1] R. L. Siegel, K. D. Miller, and A. Jemal, "Cancer statistics, 2020," *CA: a Cancer Journal for Clinicians*, vol. 70, no. 1, pp. 7–30, 2020.
- [2] F. Bray, J. Ferlay, I. Soerjomataram, R. L. Siegel, L. A. Torre, and A. Jemal, "Global cancer statistics 2018: GLOBOCAN estimates of incidence and mortality worldwide for 36 cancers in 185 countries," *CA: a Cancer Journal for Clinicians*, vol. 68, no. 6, pp. 394–424, 2018.
- [3] M. J. Schell, M. Yang, J. K. Teer et al., "A multigene mutation classification of 468 colorectal cancers reveals a prognostic role for *_APC_*," *Nature Communications*, vol. 7, no. 1, pp. 11743–11743, 2016.

- [4] R. Schulz-Heddergott, N. Stark, S. J. Edmunds et al., "Therapeutic Ablation of Gain-of-Function Mutant p53 in Colorectal Cancer Inhibits Stat3-Mediated Tumor Growth and Invasion," *Cancer Cell*, vol. 34, no. 2, pp. 298–314.e7, 2018.
- [5] W. Liao, M. J. Overman, A. T. Boutin et al., "KRAS-IRF2 Axis Drives Immune Suppression and Immune Therapy Resistance in Colorectal Cancer," *Cancer Cell*, vol. 35, no. 4, pp. 559–572.e7, 2019.
- [6] R. P. Kuiper, M. J. L. Ligtenberg, N. Hoogerbrugge, and A. Geurts van Kessel, "Germline copy number variation and cancer risk," *Current Opinion in Genetics & Development*, vol. 20, no. 3, pp. 282–289, 2010.
- [7] A. Bhan, M. Soleimani, and S. S. Mandal, "Long noncoding RNA and cancer: a new paradigm," *Cancer Research*, vol. 77, no. 15, pp. 3965–3981, 2017.
- [8] X. Deng, S. Li, F. Kong et al., "Long noncoding RNA PiHL regulates p 53 protein stability through GRWD 1/RPL 11/MDM 2 axis in colorectal cancer," *Theranostics*, vol. 10, no. 1, pp. 265–280, 2020.
- [9] X. Deng, H. Ruan, X. Zhang et al., "Long noncoding RNA CCA1 transferred from fibroblasts by exosomes promotes chemoresistance of colorectal cancer cells," *International Journal of Cancer*, vol. 146, no. 6, pp. 1700–1716, 2020.
- [10] C. Trapnell, D. G. Hendrickson, M. Sauvageau, L. Goff, J. L. Rinn, and L. Pachter, "Differential analysis of gene regulation at transcript resolution with RNA-seq," *Nature Biotechnology*, vol. 31, no. 1, pp. 46–53, 2013.
- [11] The RGASP Consortium, T. Steijger, J. F. Abril et al., "Assessment of transcript reconstruction methods for RNA-seq," *Nature Methods*, vol. 10, no. 12, pp. 1177–1184, 2013.
- [12] M. K. Iyer, Y. S. Niknafs, R. Malik et al., "The landscape of long noncoding RNAs in the human transcriptome," *Nature Genetics*, vol. 47, no. 3, pp. 199–208, 2015.
- [13] A. Subramanian, P. Tamayo, V. K. Mootha et al., "Gene set enrichment analysis: a knowledge-based approach for interpreting genome-wide expression profiles," *Proceedings of the National Academy of Sciences of the United States of America*, vol. 102, no. 43, pp. 15545–15550, 2005.
- [14] M. B. Amin, F. L. Greene, S. B. Edge et al., "The eighth edition AJCC cancer staging manual: continuing to build a bridge from a population-based to a more "personalized" approach to cancer staging," *CA: a Cancer Journal for Clinicians*, vol. 67, no. 2, pp. 93–99, 2017.
- [15] Y. H. Xing, R. W. Yao, Y. Zhang et al., "SLERT Regulates DDX21 Rings Associated with Pol I Transcription," *Cell*, vol. 169, no. 4, pp. 664–678.e16, 2017.
- [16] N. Gupta, S. S. Kupfer, and A. M. Davis, "Colorectal cancer screening," *JAMA*, vol. 321, no. 20, pp. 2022–2023, 2019.
- [17] A. L. Masson, B. A. Talseth-Palmer, T.-J. Evans et al., "Copy number variants associated with 18p11.32, *_DCC_* and the promoter 1B region of *_APC_* in colorectal polyposis patients," *Meta Gene*, vol. 7, pp. 95–104, 2016.
- [18] D. Han, M. Wang, N. Ma, Y. Xu, Y. Jiang, and X. Gao, "Long noncoding RNAs: novel players in colorectal cancer," *Cancer Letters*, vol. 361, no. 1, pp. 13–21, 2015.
- [19] H. Yari, L. Jin, L. Teng et al., "LncRNA REG1CP promotes tumorigenesis through an enhancer complex to recruit FANCD1 helicase for REG3A transcription," *Nature Communications*, vol. 10, no. 1, p. 5334, 2019.
- [20] N. Li, G. Yang, L. Luo et al., "lncRNATHAP9-AS1 Promotes pancreatic ductal adenocarcinoma growth and leads to a poor clinical outcome via sponging miR-484 and interacting with YAP," *Clinical Cancer Research: An Official Journal of the American Association for Cancer Research*, vol. 26, no. 7, pp. 1736–1748, 2020.
- [21] J. T. Hua, S. Chen, and H. H. He, "Landscape of noncoding RNA in prostate cancer," *Trends in Genetics*, vol. 35, no. 11, pp. 840–851, 2019.
- [22] M. Klingenberg, A. Matsuda, S. Diederichs, and T. Patel, "Non-coding RNA in hepatocellular carcinoma: mechanisms, biomarkers and therapeutic targets," *Journal of Hepatology*, vol. 67, no. 3, pp. 603–618, 2017.
- [23] K. E. White, B. Lorenz, W. E. Evans, T. Meitinger, T. M. Strom, and M. J. Econs, "Molecular cloning of a novel human UDP-GalNAc: polypeptide n-acetylgalactosaminyltransferase, GalNAc-t8, and analysis as a candidate autosomal dominant hypophosphatemic rickets (ADHR) gene," *Gene*, vol. 246, no. 1-2, pp. 347–356, 2000.
- [24] K. ten Hagen, T. A. Fritz, and L. A. Tabak, "All in the family: the UDP-GalNAc: polypeptide N-acetylgalactosaminyltransferases," *Glycobiology*, vol. 13, no. 1, pp. 1r–16, 2002.
- [25] P. Chai, R. Jia, R. Jia et al., "Dynamic chromosomal tuning of a novel GAU1 lncing driver at chr12p13.32 accelerates tumorigenesis," *Nucleic Acids Research*, vol. 46, no. 12, pp. 6041–6056, 2018.